Steel and Composite Structures, Vol. 10, No. 3 (2010) 245-260
DOI: http://dx.doi.org/10.12989/scs.2010.10.3.245

Buckling failure of 310 stainless steel tubes with different diameter-to-thickness ratios under cyclic bending

Kao-Hua Chang[1], Kuo-Long Lee[2] and Wen-Fung Pan[3]*

[1]*Department of Mold and Die Engineering, National Kaohsiung University of Applied Sciences Kaohsiung, Taiwan, R.O.C.*
[2]*Department of Computer Application Engineering, Far East University, Tainan County, Taiwan, R.O.C.*
[3]*Department of Engineering Science, National Cheng Kung University, Tainan, Taiwan, R.O.C.*

(Received September 14, 2009, Accepted June 4, 2010)

Abstract. In this paper, experimental and theoretical investigations on the response and collapse of 310 stainless steel tubes with different diameter-to-thickness ratios subjected to cyclic bending are discussed. The tube-bending device and curvature-ovalization measurement apparatus were used to conduct the experiment. The endochronic theory combined with the principle of virtual work and finite element software, ANSYS, were used to simulate the moment-curvature and ovalization-curvature relationships. It is shown that although the two methods lead to good simulation of the moment-curvature relationship, the endochronic theory combined with the principle of virtual work has the better simulation of the ovalization-curvature response when compared with experimental data and the simulation by ANSYS. In addition, the theoretical formulations proposed by Kyriakides and Shaw (1987) and Lee *et al*. (2001) were used to simulate the controlled curvature–number of cycles to produce buckling relationship. It is shown that the theoretical formulations effectively simulate the experimental data.

Key words: 310 stainless steel tubes; buckling failure, diameter-to-thickness ratio; cyclic bending.

1. Introduction

Stainless steel tubes 310 are frequently used as the transporting tubes for oil, gas, and water. They are also frequently used as mechanical members, such as oil-drill tube, heat exchanger tube, and bike-frame tube. These tubes are constantly subjected to cyclic bending. It is well known that the ovalization of the tube cross-section (change of the outside diameter / original outside diameter, $\Delta D_o/D_o$) is observed when a circular tube is subjected to bending. If the loading history is cyclic bending, the ovalization increases in a ratcheting manner with the number of cycles. Increase in ovalization causes a progressive reduction in the bending rigidity, which can result in buckling of the tube components. Therefore, the experimental and theoretical studies of the response and collapse of 310 stainless steel tubes under cyclic bending are of importance in many industrial applications.

It has been found that a lot of metal tubes have been studied such as: 6061-T6 aluminum alloy tube (Kyriakides and Shaw 1987, Corona *et al*. 2006), 7005-T51 aluminum alloy tube (Lee *et al*. 2010), Ti-

* Corresponding author, Professor, E-mail: pan@phoebus.es.ncku.edu.tw

2Al-Cb-Ta titanium alloy tube (Hsu *et al*. 2000, Lee *et al*. 2010), 70:30 brass tube (Lee *et al*. 2010), 1018 steel tube (Kyriakides and Shaw 1987), 1020 steel tube (Corona and Kyriakides 1991, Kyriakides *et al*. 2008), grade C350 steel tube (Elchalakani *et al*. 2002), VHS steel tubes (Jiao and Zhao 2004), 321 stainless steel (Limam *et al*. 2008), 304 stainless steel tube (Corona and Kyriakides 1988, Corona and Kyriakides 2000, Lee *et al*. 2004, Chang *et al*. 2008, Lee *et al*. 2010), 316L stainless steel tube (Lee *et al*. 2005, Chang *et al*. 2005, Lee *et al*. 2010), cold-formed circular steel tube (Elchalakani *et al*. 2006, Elchalakani and Zhao 2008). However, a very important metal tube "310 stainless steel tubes", which are constantly used by industry, is lack of investigation.

In this study, a tube-bending device (Shaw and Kyriakides 1985, Kyriakides and Shaw 1987, Pan and Her 1998, Lee *et al*. 2001) was used to conduct the cyclic bending tests for 310 stainless steel tube with four different diameter-to-thickness ratios (D_o/t ratios) of 60, 50, 40 and 30. The magnitude of bending moment was measured using two load cells, mounted in the tube-bending device, and the magnitudes of the curvature and the ovalization of the tube cross-section were measured using the curvature-ovalization measurement apparatus which was designed and reported previously by Pan *et al*. (1998). The number of cycles to produce buckling was also recorded.

The simulation of moment-curvature and ovalization-curvature relationships was first proposed by Kyriakides and Shaw (1982). The major structure of their method as shown Fig. 1 is used to build the kinematics of the circular tube under pure bending. Next, a plasticity model is used to describe the elastoplastic behavior of the material. A group of Fourier series is used to describe the circumferential displacements of the tube. By combining with the principle of virtual work, a system of nonlinear algebraic equations is determined. This system of equations can be solved by numerical method. They used this method to simulate the responses of several metal tubes (Kyriakides and Shaw 1982, Shaw and Kyriakides 1985, Corona and Kyriakides 1988, Corona and Kyriakides 2000, Corona *et al*. 2006). Pan and his co-workers also used a similar method, but they selected the endochronic theory for describing the elastoplastic response of the tube. Various kinds of metal tubes were investigated (Lee and Chang 2004, Lee *et al*. 2004, Lee *et al*. 2005, Chang *et al*. 2005, Chang *et al*. 2008, Lee *et al*. 2008, Lee *et al*. 2010).

In this theoretical study, the endochronic theory combined with the principle of virtual work was used to simulate the moment-curvature and ovalization-curvature responses of 310 stainless steel tubes under cyclic bending. In addition, due to the great progress in computation speed and great improvement in the

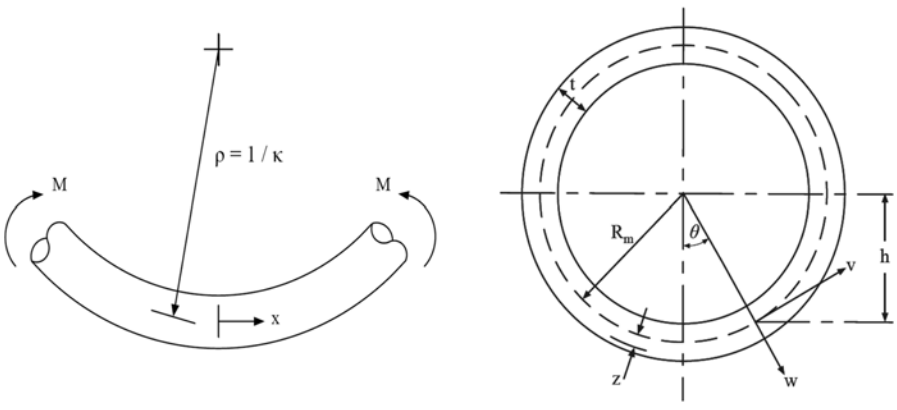

Fig. 1 Problem geometry of circular tube subjected to pure bending

theory for describing the elastoplastic response in finite element method in recent years, the accuracy of calculation by finite element method gets better. In this study, the finite element software, ANSYS, was used to simulate the aforementioned relationships. It is shown that the two methods lead to good simulation of moment-curvature relationship. However, the endochronic theory combined with the principle of virtual work has the best simulation of the ovalization-curvature response when compared with the experimental data and the simulations by ANSYS.

Next, it can be observed that although four different D_o/t ratios of tested tube, four almost parallel lines can be seen from the relationship between the controlled curvature and the number of cycles to produce buckling in the log-log scale. This phenomenon is similar to that of 304 stainless steel tube discovered by Lee *et al*. (2001). The empirical formula proposed by Kyriakides and Shaw (1987) and Lee *et al*. (2001) were used for simulating the relationship between the controlled curvature and the number of cycles to produce buckling of 310 stainless steel tubes with different D_o/t ratios under cyclic bending. The theoretical and experimental results are found to be in good agreement.

2. Experimental facility, material, specimens and test procedures

In this study, the cyclic bending experiments on 310 stainless steel tubes were conducted using a tube-bending device and a curvature-ovalization measurement apparatus. Detailed descriptions of the device, apparatus, materials and test procedures are stated in the following.

2.1 Tube-bending device

A schematic drawing of the tube-bending device is shown in Fig. 2. It is designed as a four-point bending machine, capable of applying reverse cyclic bending. The device consists of two rotating sprockets resting on two support beams. Heavy chains run around the sprockets resting on two heavily supported beams 1.25 m apart. This allows the maximum length of test specimen to be 1 m. The bending capacity of the machine is 5300 N-m. Each tube is tested and fitted with a solid rod extension. The contact between the tube and the rollers is free to move along the axial direction during bending. The load transfer to the test specimen is formed by concentrated loads from two of the rollers in the form of a couple. Once either the top or bottom cylinder is contracted, the sprockets are rotated, and

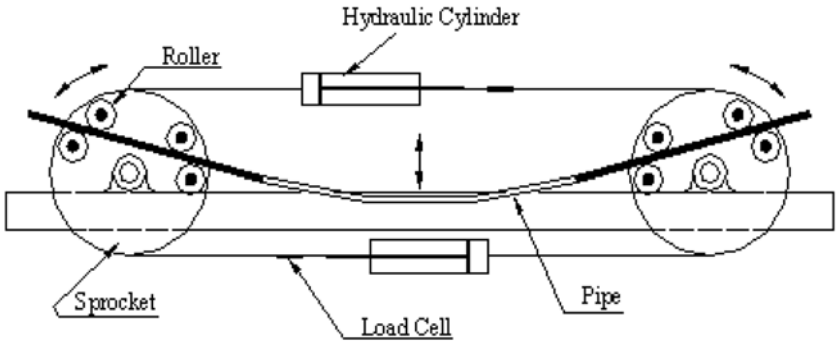

Fig. 2 Schematic drawing of the tube-bending device

pure bending of the test specimen is achieved. Reverse bending can be achieved by reversing the flow direction in the hydraulic circuit (Shaw and Kyriakides 1985, Kyriakides and Shaw 1987, Pan and Her 1998, Lee *et al*. 2001, Chang and Pan 2009).

2.2 Curvature-ovalization measurement apparatus (COMA)

The COMA is an instrument used for measuring the tube curvature and ovalization of a tube cross-section. Fig. 3 shows a schematic drawing of COMA. It is a lightweight instrument, which can be mounted close to the tube mid-span. There are three inclinometers in the COMA. Two inclinometers are fixed on two holders, which are denoted as side-inclinometers (see Fig. 3). These holders are fixed on the circular tube before the test begins. Based on the fixed distance between the two side-inclinometers and the angle changes detected by the two side-inclinometers, the tube curvature can be obtained by simple calculation. In addition, by using the magnetic detector on the middle part of COMA to measure the change of outside diameter, the ovalization of the tube cross-section can be determined. A detailed description of the tube-bending device and the COMA can be found in Pan *et al*. (1998).

2.3 Material

Circular tubes made of 310 stainless steel have been used in this study. The tube's chemical composition (in mass percentages) is Cr (24.42%), Ni (19.37%), Mn (2.12%), Si (1.75%), …, and the remainder Fe. The 0.2% proof stress of 310 stainless steel was 292 MPa, and its ultimate tensile stress was 617 MPa with a 45% percent elongation.

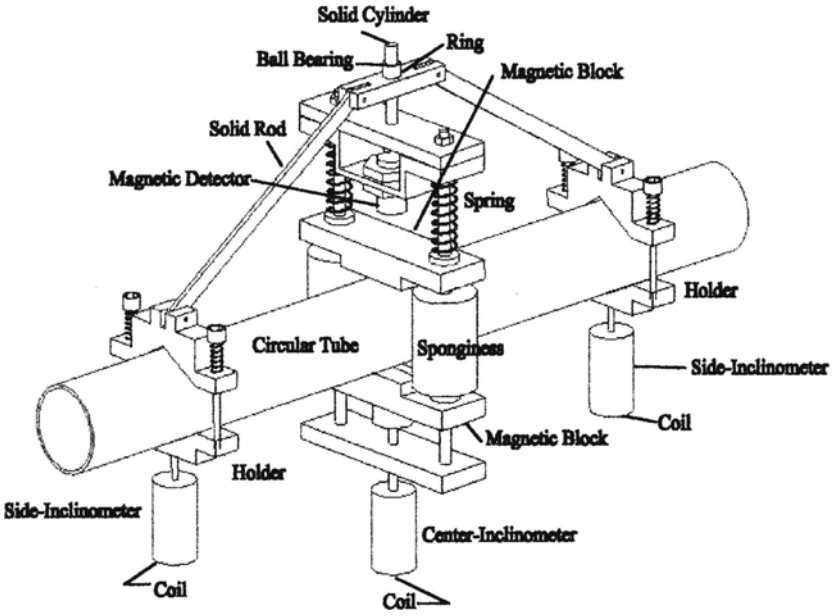

Fig. 3 Schematic drawing of the COMA

2.4 Specimens

The 310 stainless steel tubes with D_o of 38.1 mm and t of 1.5 mm were slightly machined on the outside diameter to obtain the desired D_o/t ratios of 60, 50, 40 and 30, respectively. Note that the process of machining tubes is the same as that used by Lee *et al*. (2001).

2.5 Experimental procedure

In this study, cyclic bending test was conducted by using the tube-bending device described in Section 2.1. The experiment was the curvature-controlled cyclic bending test. The magnitude of the curvature was controlled and measured by COMA, which also measured the ovalization of tube cross-section. The bending moment can be calculated from the signals detected by the two load cells mounted on the tube-bending device. In addition, the number of cycles to produce buckling was also being recorded. Fig. 4 demonstrates the schematic drawing of the controlled curvature (κ_c) versus time for curvature-controlled cyclic bending history. The counting of one cycle is also indicated in this figure.

3. Experimental and theoretical results of the mechanical response

3.1 Experimental mechanical response for 310 stainless steel tubes under cyclic bending

Figs. 5(a)-(d) shows typical experimental results of cyclic moment (M) - curvature (κ) curve for 310 stainless steel tubes with different D_o/t ratios of 60, 50, 40 and 30, respectively. The controlled minimum and maximum values of curvature are −0.3 and 0.3 m^{-1}, respectively. It is observed from the M-κ curve for all D_o/t ratios that the 310 stainless steel tubes exhibit cyclic hardening and become gradually steady after a few cycles for symmetric curvature-controlled cyclic bending. A tube with a higher D_o/t ratio has a smaller size of wall-thickness. Thus, a lower magnitude of the moment is needed when the tube bends to the maximum curvature at 0.3 m^{-1}. Figs. 6(a)-(d) shows the corresponding experimental results for the cyclic ovalization ($\Delta D_o/D_o$) - curvature (κ) curve. The ovalization is seen to be continuously changing. On first loading, the ovalization grows to a maximum value at the controlled maximum curvature. On unloading to zero curvature, some permanent deformation of the tube cross-section is observed. Continuous reverse bending to the minimum curvature causes the ovalization to increase again. The ovalization increases in a symmetric and ratcheting manner with the number of

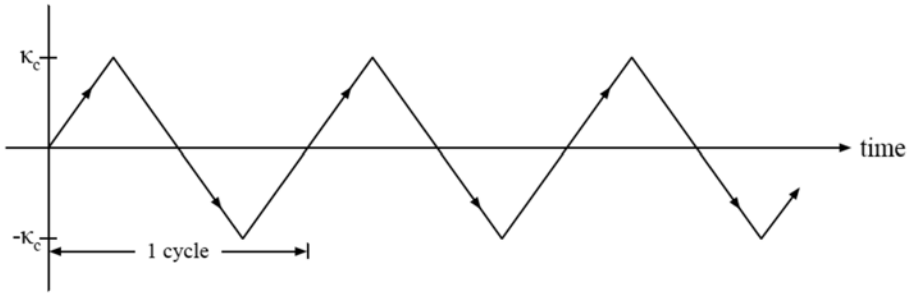

Fig. 4 Schematic drawing of the controlled curvature (κ_c) versus time for curvature-controlled cyclic bending history

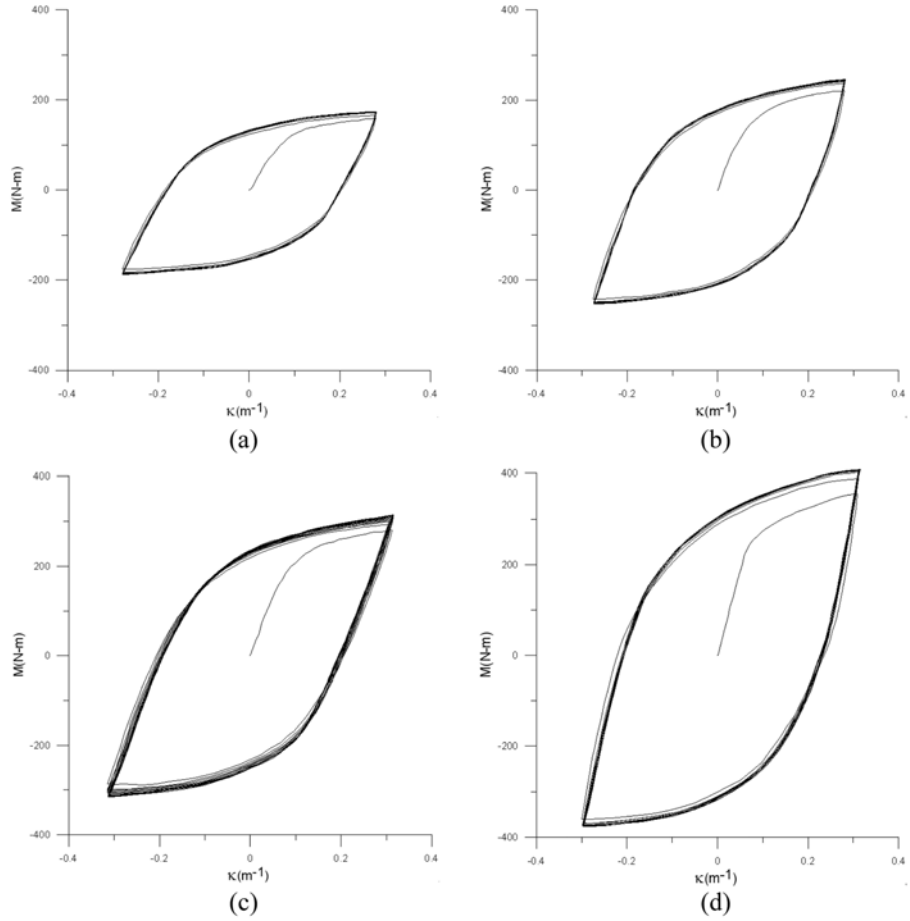

Fig. 5 Experimentally determined cyclic moment (M) - curvature (κ) for 310 stainless steel tubes with different D_o/t ratios of (a)60, (b)50, (c)40 and (d)30

bending cycles. The ovalization continues to progress until a certain critical value is achieved at which the tube buckles. It is seen that the higher the D_o/t ratio, the faster the accumulation of the ovalization in the tube cross-section.

3.2 Endochronic theory combined with the principle of virtual work

The major structure of the method is to use Fig. 1 to build the kinematics of circular tube under cyclic bending. The first-order ordinary differential constitutive equations of the endochronic theory derived by Pan and Chern (1997) are used for the description of the elastoplastic behavior of the tube. A group of Fourier series ($\sum_{n=0}^{N} a_n \sin n\theta$ and $\sum_{n=0}^{N} b_n \cos n\theta$) is used to describe the circumferential displacements of the tube. By combining with the principle of virtual work, a system of nonlinear algebraic equations is determined. This system of equations can be solved by Newton-Raphson method. A detailed description of the method is found in several papers (Lee *et al*. 2001, Lee *et al.* 2004, Chang *et al*. 2008,

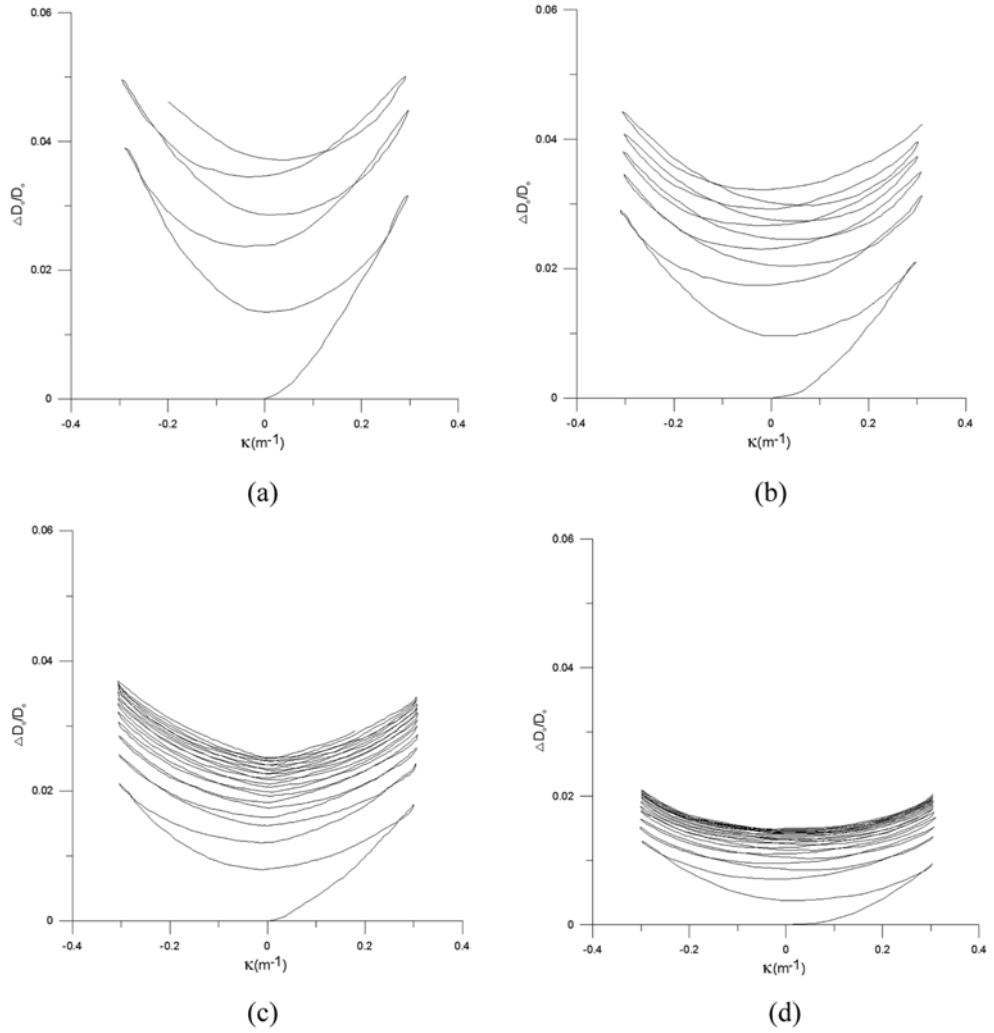

Fig. 6 Corresponding experimental results for the cyclic ovalization ($\Delta D_o/D_o$) - curvature (κ) curve for 310 stainless steel tubes with different D_o/t ratios of (a)60, (b)50, (c)40 and (d) 30

Lee *et al*. 2010). According to the method proposed by Fan (1983), the material parameters of 310 stainless steel were determined to be: $\mu_0 = 72$ GPa, $K = 154$ GPa, $C_1 = 4.85 \times 10^6$ MPa, $\alpha_1 = 8730$, $C_2 = 5.46 \times 10^5$ MPa, $\alpha_2 = 960$, $C_3 = 4.7 \times 10^4$ MPa, $\alpha_3 = 170$. Since the simulation of the moment-curvature behavior by the finite element method did not consider the cyclic hardening phenomenon, the endochronic theory also ignored the cyclic hardening phenomenon. Thus, the material function in the endochronic theory should be equal to one. The values of the material parameters C and β in material function were zero (Pan and Chern 1997).

3.3 Finite element method ANSYS

Due to the symmetry of the tube, only half of the tube was considered in this analysis. Figs. 7(a) and

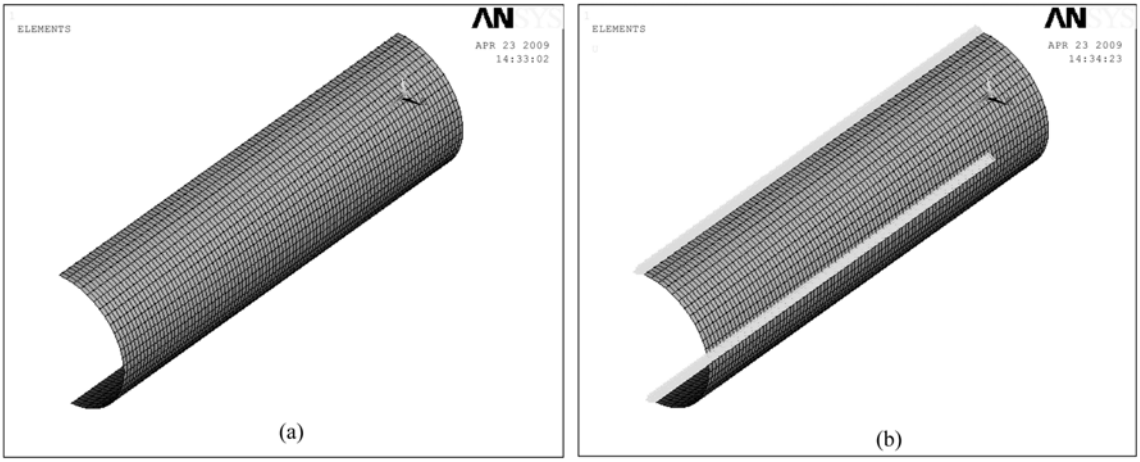

Fig. 7 (a) Mesh and (b) boundary condition of the finite element method ANSYS

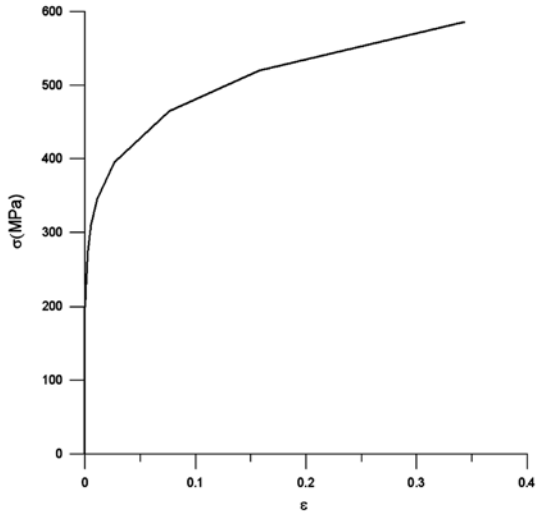

Fig. 8 Multilinear segments of the stress-strain relationship for 310 stainless steel

(b) demonstrates the mesh and boundary condition of the finite element method ANSYS, respectively. As for the material elastoplastic behavior, the multilinear segments of the stress-strain relationship for 310 stainless steel as shown in Fig. 8 were considered in this case. The hardening rule used was the kinematic hardening rule.

3.4 Comparison of the theoretical and experimental results

Fig. 9(a) shows the experimental cyclic moment (M) - curvature (κ) curve for 310 stainless steel tubes with the D_o/t ratio of 60. The loading condition is the same as the case in Fig. 5(a). Figs. 9(b) and 9(c) show the corresponding theoretical analyses by the endochronic theory combined with the principle of

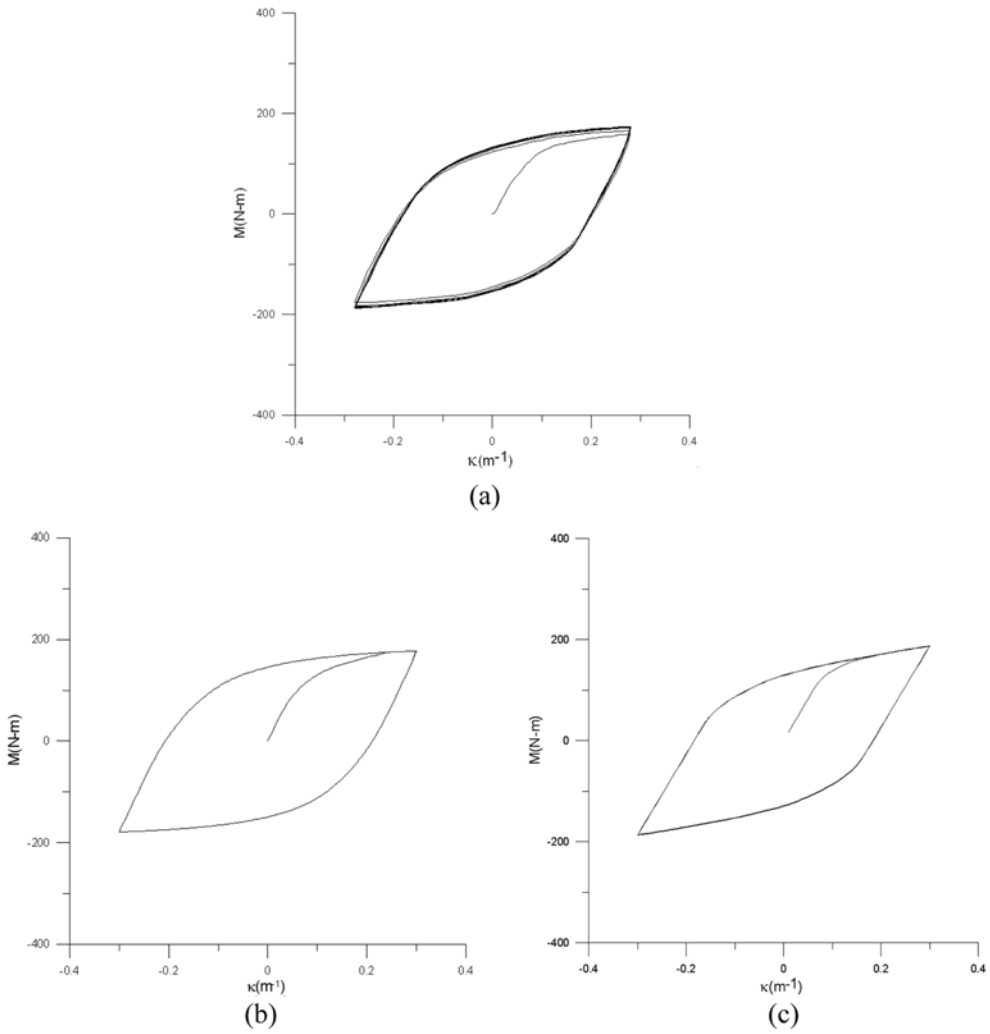

Fig. 9 Cyclic moment (M) - curvature (κ) for 310 stainless steel tubes with the D_o/t ratio of 60. (a) Experiment result, (b) theoretical analysis by the endochronic theory combined with the principle of virtual work, and (c) theoretical analysis by ANSYS

virtual work and the finite element method ANSYS, respectively. In general, two theoretical analyses can very well simulate the M-κ response. Similar outcome is found in Figs. 10(a)-(c) for 310 stainless steel tubes with the D_o/t ratio of 50. Due to similar results, the theoretical simulations of the M-κ response for 310 stainless steel tubes with the D_o/t ratios of 40 and 30 do not show in this paper.

Fig. 11(a) shows the experimental cyclic ovalization ($\Delta D_o/D_o$) - curvature (κ) curve for 310 stainless steel tubes with the D_o/t ratio of 60. Figs. 11(b) and 11(c) show the corresponding theoretical analyses by the endochronic theory combined with the principle of virtual work and the finite element method ANSYS, respectively. It can be seen that the simulations by these two methods have some deviation from the experimental data, but the theoretical analysis by the endochronic theory provides the better result when compared with the finite element method ANSYS and the experimental data. Similar

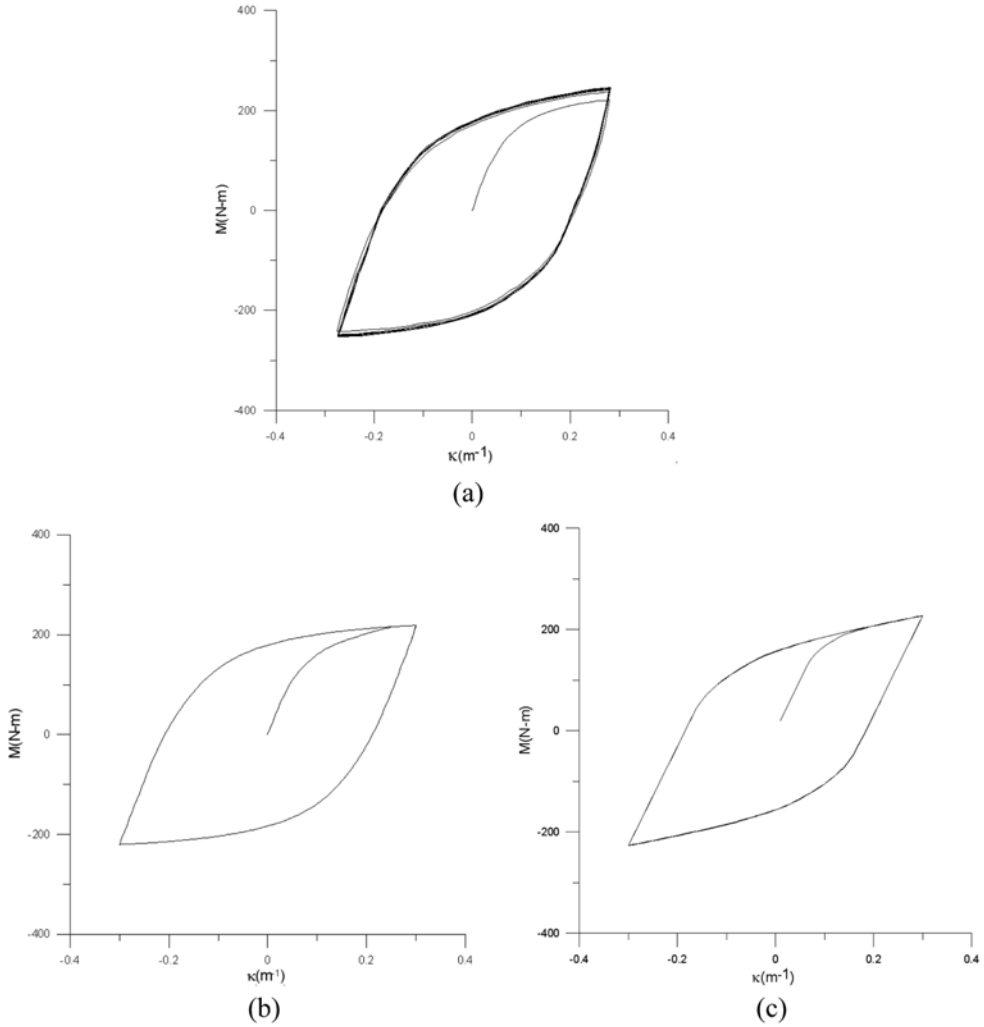

Fig. 10 Cyclic moment (M) - curvature (κ) for 310 stainless steel tubes with the D_o/t ratio of 50. (a) Experiment result, (b) theoretical analysis by the endochronic theory combined with the principle of virtual work, and (c) theoretical analysis by ANSYS

outcome is found in Fig. 12(a)-(c) for 310 stainless steel tubes with the D_o/t ratio of 50. Theoretical simulations of the $\Delta D_o/D_o$-κ response for 310 stainless steel tubes with the D_o/t ratios of 40 and 30 aren't shown in this paper because of similar results.

4. Collapse of 310 stainless steel tubes under cyclic bending

Fig. 13 shows the experimental results of the controlled curvature (κ_c) versus the number of cycles necessary to produce buckling (N_b) for 310 stainless steel tubes with the D_o/t ratios of 60, 50, 40 and 30. The magnitudes of κ_c vary from ± 0.2 to ± 0.7 m^{-1}. It can also be seen from Fig. 13 that for a certain

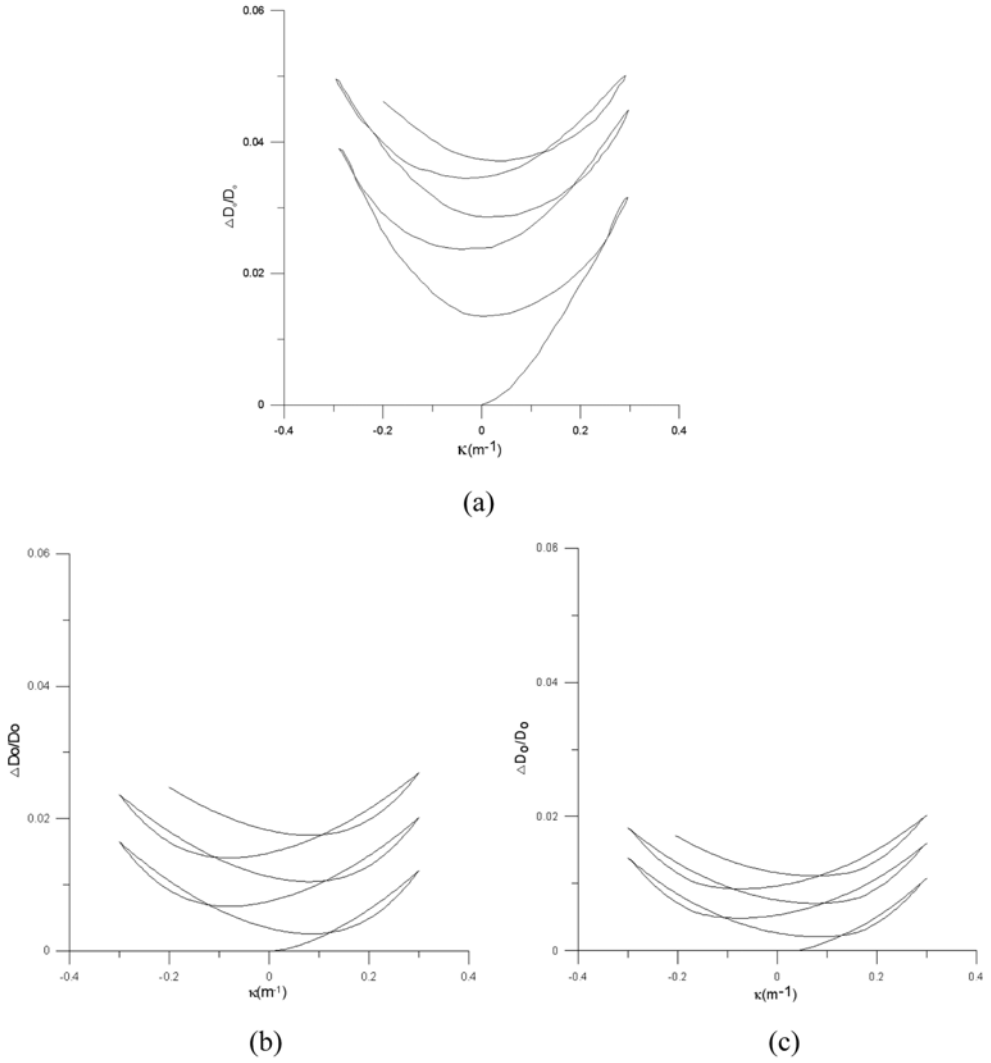

Fig. 11 Cyclic ovalization ($\Delta D_o/D_o$) - curvature (κ) for 310 stainless steel tubes with the D_o/t ratio of 60. (a) Experiment result, (b) theoretical analysis by the endochronic theory combined with the principle of virtual work, and (c) theoretical analysis by ANSYS

amount of κ_c, the tube with a higher D_o/t ratio leads to a lower number of cycles necessary to produce buckling. The same results of Fig. 13 are plotted on a log-log scale and are shown in Fig. 14. The four straight lines in this figure, determined by the least square method, denote four different D_o/t ratios of tubes. Although four groups of tested specimens had four different D_o/t ratios, four almost parallel straight lines could be seen. This phenomenon is also seen by Lee *et al*. (2001) for 304 stainless steel tubes with four different D_o/t ratios.

In 1987, Kyriakides and Shaw (1987) proposed the relationship between the κ_c and N_b as

$$\kappa_c = C\ (N_b)^{-\alpha} \tag{1}$$

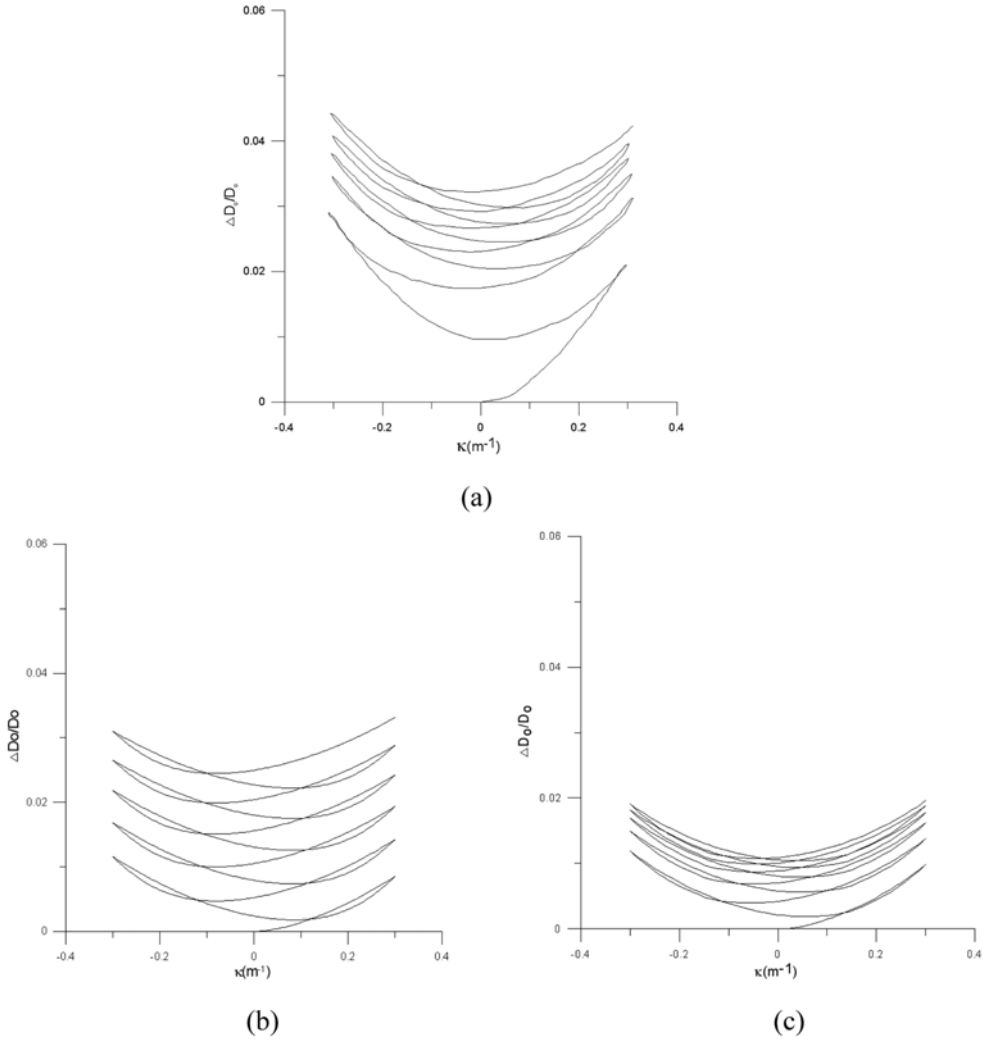

Fig. 12 Cyclic ovalization ($\Delta D_o/D_o$) - curvature (κ) for 310 stainless steel tubes with the D_o/t ratio of 50. (a) Experiment result, (b) theoretical analysis by the endochronic theory combined with the principle of virtual work, and (c) theoretical analysis by ANSYS

where C and α are material parameters, which are related to the material properties and the D_o/t ratio. The constant C is the magnitude of cyclic curvature at $N_b = 1$ and α is the slope on the log-log plot. In 2001, Lee *et al*. (2001) studied the influence of the D_o/t ratio on the stability of circular tubes subjected to cyclic bending. They proposed a formulation for the material parameter C to be the function of the D_o/t ratio, which is

$$C = C_0 \, (D_o/t)^{-\gamma} \tag{2}$$

where C_0 and γ are material parameters. They investigated the 304 stainless steel tubes with different D_o/t ratios under cyclic bending. The material parameters C_0 and γ were determined to be 95.1 m^{-1} and

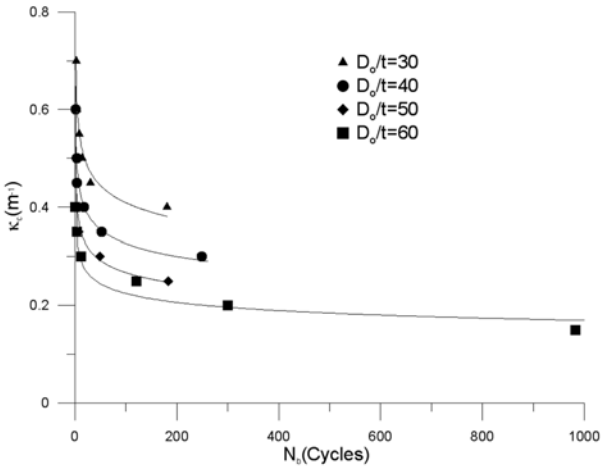

Fig. 13 Experimental results of the controlled curvature (κ_c) versus the number of cycles necessary to produce buckling (N_b) for 310 stainless steel tubes with the D_o/t ratios of 60, 50, 40 and 30

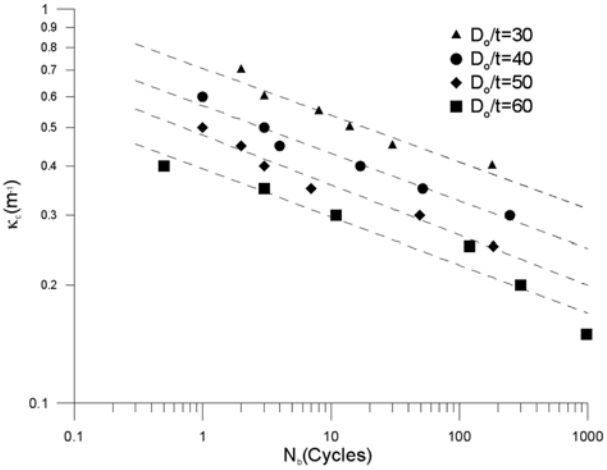

Fig. 14 Experimental results of the controlled curvature (κ_c) versus the number of cycles necessary to produce buckling (N_b) for 310 stainless steel tubes with the D_o/t ratios of 60, 50, 40 and 30 on a log-log scale

1.406. Eqs. (1) and (2) were used for simulate the κ_c-N_b response of 310 stainless steel tubes with different D_o/t ratios subjected to cyclic bending. As shown in Fig. 15, the material parameters C_0 and γ for 310 stainless steel tubes were determined to be 46.3 m^{-1} and 1.232, respectively. The material parameter of α is 0.121. Fig. 16 shows the experimental and simulated results. Good agreement between the theoretical simulation and experimental finding has been achieved.

5. Conclusions

In this study, the response and collapse of 310 stainless steel tubes with different D_o/t ratios were

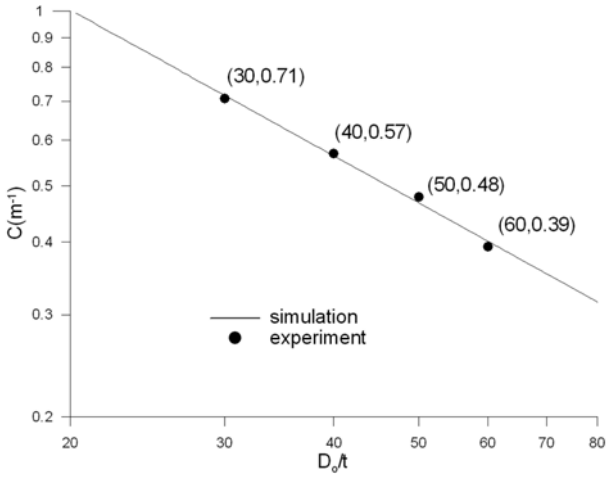

Fig. 15 Relationship between C and D_o/t ratios

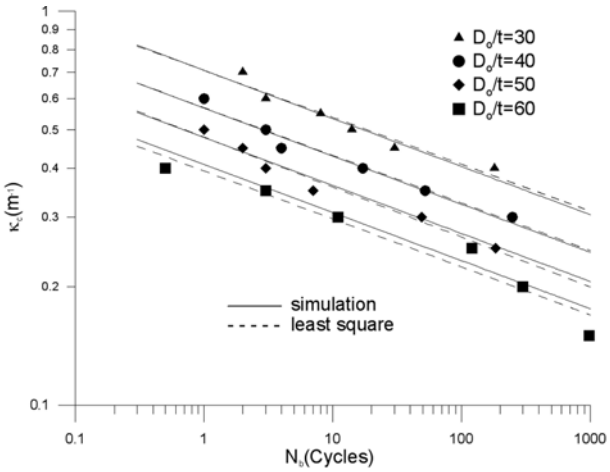

Fig. 16 Experimental and theoretical results of the controlled curvature (κ_c) versus the number of cycles necessary to produce buckling (N_b) for 310 stainless steel tubes with the D_o/t ratios of 60, 50, 40 and 30 on a log-log scale

investigated. According to the experimental and theoretical results, the following important conclusions are apparent from this investigation:

(1) For symmetric curvature-controlled cyclic bending, the M – κ loop of the 310 stainless steel tube shows cyclic hardening. But the loops become gradually steady after a few cycles. The $\Delta D_o/D_o$ – κ curve shows the increased ratcheting with the number of cycles. Moreover, persistent cycling eventually leads to buckling.

(2) The two theoretical methods revealed a good simulation for the M-κ response. However, for the $\Delta D_o/D_o$ – κ response, the theoretical analysis by the endochronic theory combined with the principle of virtual work leads to the better simulation when compared with the finite element methods ANSYS and experimental data.

(3) It can also be seen that for a certain amount of κ_c, the tube with a higher D_o/t ratio leads to a lower number of cycles necessary to produce buckling. Although four groups of tested specimens had four different D_o/t ratios (60, 50, 40 and 30), four almost parallel straight lines could be seen for κ_c-N_b curves plotted on a log-log scale. Finally, the theoretical formulations proposed by Kyriakides and Shaw (1987) and Lee *et al*. (2001) were used for simulating the aforementioned response. The material parameters A_0, γ and α were determined to be 46.3 m^{-1}, 1.232 and 0.121, respectively. Good agreement between the theoretical and experimental results has been achieved.

6. Acknowledgements

The work presented was carried out with the support of the National Science Council under grant NSC 94-2212-E-006-061. Its support is gratefully acknowledged.

References

Chang, K.H. and Pan, W.F. (2009), "Buckling life estimation of circular tubes under cyclic bending", *Int. J. Solids. Struct.*, **46**(2), 254-270.

Chang, K.H., Pan, W.F. and Lee, K.L. (2008), "Mean moment effect on circular thin-walled tubes under cyclic bending", *Struct. Eng. Mech.*, **28**(5), 495-514.

Chang, K.H., Hsu, C.M., Sheu, S.R. and Pan, W.F. (2005), "Viscoplastic response and collapse of 316L stainless steel tubes under cyclic bending", *Steel. Compos. Struct.* **5**(5), 359-374.

Corona, E. and Kyriakides, S. (1988), "On the collapse of inelastic tubes under combined bending and pressure", *J. Eng. Mech.*, **120**(12), 1232-1239.

Corona, E. and Kyriakides, S. (2000), "Asymmetric collapse modes of pipes under combined bending and pressure", *Int. J. Solids. Struct*., **24**(5), 505-535.

Corona, E., Lee, L.H. and Kyriakides, S. (2006), "Yield anisotropic effects on buckling of circular tubes under bending", *Int. J. Solids. Struct.*, **43**(22-23), 7099-7118.

Elchalakani, M. and Zhao, X.L. (2008), "Concrete-filled cold-formed circular steel tubes subjected to variable amplitude cyclic pure bending", *Eng. Struct.*, **30**(2), 287-299

Elchalakani, M., Zhao, X.L. and Grzebieta, R.H. (2002), "Plastic mechanism analysis of circular tubes under pure bending", *Int. J. Mech. Sci.*, **44**(6), 1117-1143.

Elchalakani, M., Zhao, X.L. and Grzebieta, R.H. (2006), "Variable amplitude cyclic pure bending tests to determine fully ductile section slenderness limits for cold-formed CHS", *Eng. Struct.*, **28**(9), 1223-1235

Fan, J. (1983), "A comprehensive numerical study and experimental verification of endochronic plasticity", Ph.D. Dissertation, Department of Aerospace Engineering and Applied Mechanics, University of Cincinnati.

Hsu, C.M., Chiou, S.B. and Chang, Y.S. (2000), "Inelastic response and stability of titanium alloy tubes under cyclic bending", *JSME Int.J.A-Solid.M.*, **43**(1), 63-68.

Jiao, H. and Zhao, X.L. (2004), "Section slenderness limits of very high strength circular steel tubes in bending", *Thin. Wall. Struct.*, **42**(9), 1257-1271.

Kyriakides, S., Ok, A. and Corona, E. (2006), "Localization and propagation of curvature under pure bending in steel tubes with Lüders bands", *Int.J.Solids.Struct.*, **45**, 3074-3087.

Kyriakides, S. and Shaw, P.K. (1982), "Response and stability of elastoplastic circular pipes under combined bending and external pressure", *Int.J.Solids.Struct.*, **18**(11), 957-973.

Kyriakides, S. and Shaw, P.K. (1987), "Inelastic buckling of tubes under cyclic loads", *J. Press.Vess-T.ASME.*, **109**, 169-178.

Lee, K.L. and Chang, K.H. (2004), "Endochronic simulation for viscoplastic collapse of long, thick-walled tubes subjected to external pressure and axial tension", *Struct. Eng. Mech.*, **18**(5), 627-644.

Lee, K.L., Pan, W.F. and Kuo, J.N. (2001), "The influence of the diameter-to-thickness ratio on the stability of circular tubes under cyclic bending", *Int. J. Solids. Struct.*, **38**(14), 2401-2413.
Lee, K.L., Pan, W.F. and Hsu, C.M. (2004), "Experimental and theoretical evaluations of the effect between diameter-to-thickness ratio and curvature-rate on the stability of circular tubes under cyclic bending", *JSME Int.J.A-Solid.M.*, **47**(2), 212-222.
Lee, K.L., Shie, R.F. and Chang, K.H. (2005), "Experimental and theoretical investigation of the response and collapse of 316L stainless steel tubes subjected to cyclic bending", *JSME Int.J.A-Solid.M.*, **48**(3), 155-162.
Lee, K.L., Hsu, C.M. and Chang, K.H. (2008), "Endochronic simulation for the response of 1020 carbon steel under symmetric and unsymmetric cyclic bending with or without external pressure", *Steel. Compos. Struct.* **8**(2), 99-114.
Lee, K.L., Hung, C.Y. and Pan, W.F. (2010), "Buckling life estimation of circular tubes of different materials under cyclic bending", *J. Chin. Ins. Eng.*, **33**(2), 177-189.
Limam, A., Lee, L.H., Corana, E. and Kyriakides, S. (2008), "Plastic buckling and collapse of tubes under bending and internal pressure", *Proceeding of the 27th international Conference on Offshore Mechanics and Arctic Engineering*, June, Estoril, Portugal.
Pan, W.F. and Chern, C.H. (1997), "Endochronic description for viscoplastic behavior of materials under multiaxial loading", *Int. J. Solids. Struct.*, **34**(17), 2131-2160.
Pan, W.F., Wang, T.R. and Hsu, C.M. (1998), "A curvature-ovalization measurement apparatus for circular tubes under cyclic bending", *Exper. Mech.*, **38**(2), 99-102.
Pan, W.F. and Her, Y.S. (1998), "Viscoplastic collapse of thin-walled tubes under cyclic bending", *J. Eng.Mater-T.ASME.*, 120, 287-290.
Shaw, P.K. and Kyriakides, S. (1985), "Inelastic analysis of thin-walled tubes under cyclic bending", *Int. J. Solids. Struct.*, **21**(11), 1073-1110.

CC